Sensors **2007**, *7*, 3329-3346

sensors

ISSN 1424-8220

www.mdpi.org/sensors

Full Research Paper

pH Sensitivity of Novel PANI/PVB/PS3 Composite Films

Edric Gill [1], Arousian Arshak [1,*], Khalil Arshak [2] and Olga Korostynska [2]

1 Dept. of Physics, University of Limerick, Limerick, Ireland.
Tel: +353 61 20 2371, Fax: +353 61 20 2423
2 Dept. of Computer and Electronic Engineering, University of Limerick, Limerick, Ireland

* Author to whom correspondence should be addressed. E-mail: Arousian.Arshak@ul.ie

Received: 29 November 2007 / Accepted: 18 December 2007 / Published: 19 December 2007

Abstract: This paper reports on the results from the investigation into the pH sensitivity of novel PANI/PVB/PS3 composite films. The conductimetric sensing mode was chosen as it is one of the most promising alternatives to the mainstream pH-sensing methods and it is the least investigated due to the popularity of other approaches. The films were deposited using both screen-printing and a drop-coating method. It was found that the best response to pH was obtained from the screen-printed thick films, which demonstrated a change in conductance by as much as three orders of magnitude over the pH range pH2-pH11. The devices exhibited a stable response over 96 hours of operation. Several films were immersed in buffer solutions of different pH values for 96 hours and these were then investigated using XPS. The resulting N 1s spectra for the various films confirmed that the change in conductance was due to deprotonation of the PANI polymer backbone. SEM and Profilometry were also undertaken and showed that no considerable changes in the morphology of the films took place and that the films did not swell or contract due to exposure to test solutions.

Keywords: PANI composite film, XPS, thick films, conductance, interdigitated electrodes.

1. Introduction

Sensors to measure pH are amongst the most widely used chemical sensing devices available today. These devices have found uses in many different industries, from pollution measurement and control [1], to miniaturized medical biosensors [2]. With advances in the semiconductor fabrication industry

and in polymer technology, considerable research has been conducted in the area of pH sensing techniques using polymer-based sensing layers [3-7].

Conducting polymers are novel materials that exhibit low electrical resistivity, unlike other polymer substances that are highly insulating in nature. Researchers were familiar with conducting polymers in their non-conducting forms for some time before their high conductivity states were discovered [8]. Several pH sensors have been produced using these materials [9-13]. Polyaniline (PANI), in particular, has proven to be the most promising conducting polymer in terms of pH-sensing applications, due to the fact that the conductivity of a PANI film varies considerably in solutions of different pH. PANI is the most studied conducting polymer since it was first reported as early as 1862 [14]. More detailed research into PANI was not conducted until nearly a century later, when it was realized how wide the potential applications of such a novel material could be.

Polyaniline has been reported as part of the sensing layers of many devices, detecting parameters such as glucose [15-17] and urea [18-20] concentration; and cholesterol levels [21-23]. Other novel sensors capable of detecting bacteria [23] and other potentially harmful organisms have also used PANI in the sensing layers. However, pH sensors using the conductimetric measurement mode in conjunction with PANI as a functional material have not been reported extensively in the literature. There are many reasons for this, including the huge popularity of the pre-existent potentiometric pH sensing technology. However, PANI composites show potential in this area and can be exploited. This work shows the response of such a sensor to changes in pH.

The main reasons that PANI is a popular choice for such applications are its wide conductivity range (doping dependent) and the ease with which it can be cast into a film. PANI can be used as a pH-sensitive layer, the reason being the unique chemical structure of the material.

PANI can be found in several oxidation states, which are dependent on both potential and pH [25]. PANI has three generally agreed upon base forms: Pernigraniline (PNB) that is fully oxidized, Emeraldine (EB) that is half-oxidized, and Leucoemeraldine (LEB) that is fully oxidized [26]. In this work, the pH-sensitivity of emeraldine salt (ES) (the conducting form of EB) is investigated.

ES PANI has a relatively high conductivity (up to 10^2 S/cm [27]) under the correct doping conditions. By adding protons to the backbone of the polymer, the material becomes electrically conducting. Figure 1 shows both the protonated (ES) and unprotonated (EB) forms of emeraldine PANI and the reactions that can cause such a change in the conductance of the material [25, 28]. This doping method changes the overall structure of the polymer, however, there is no change in the overall number of electrons in the system. It is generally accepted [29, 30] that the enhanced electrical conductivity which is observed after doping EB (to form ES) arises from the polarons and bipolarons which are formed during the doping process and are the charge carriers in the system. The protonation takes place on the imine nitrogen sites, and, the resulting structure resembles that of a bipolaron lattice. This topic has been dealt with in some detail in the paper by Ray *et al.* [31].

When an ES film is placed into an alkaline solution, the film becomes deprotonated and the conductivity of the films undergoes a dramatic decrease in magnitude. When the film is placed into an acidic solution, the conductivity of the film returns to a higher value due to the reprotonation of the backbone of the polymer. The reason for this unusual characteristic is the presence of basic sites (amine and imine groups) in the polymer structure, as shown in Figure 1. It is this strong pH-

dependence that makes PANI one of the most suitable materials to act as a pH-sensitive layer in any pH sensor.

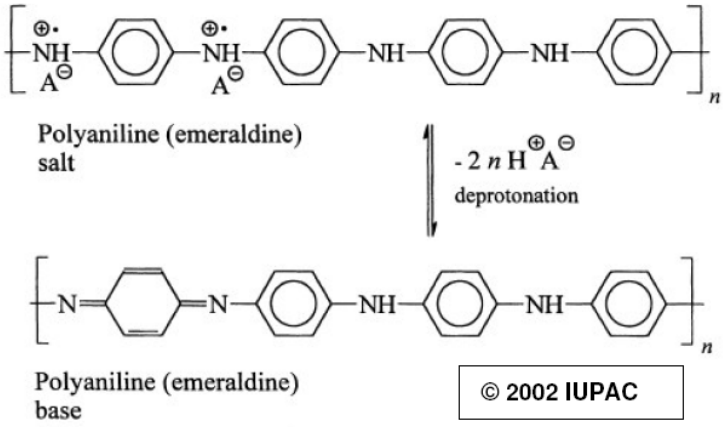

Figure 1. Polyaniline (emeraldine) salt is deprotonated in the alkaline medium to polyaniline (emeraldine) base. [A^- is an arbitrary anion, e.g. chloride]. [28]

One of the main contributors to research involving PANI in this capacity is Lindfors *et al.* [25, 32-35]. In their work, the researchers report on using PANI in three different pH-measurement modes: potentiometric [32], optical [33] and Raman [34, 35]. The results obtained from the research are extremely positive in terms of the applicability of PANI in such applications, with each approach producing an excellent response to pH. An important finding from this research is the solution to the problem of hysteresis (memory effect) that can become a problem when investigating PANI in such an application.

The main advantage of the approach detailed in this paper is that the entire measurement can be miniaturized for portable applications, unlike many of the optical techniques that require bulky equipment and are therefore not portable.

2. Experimental Section

In this work, both thick film and a drop coating approach were utilized. The thick film screen-printing technique was chosen, as it is cost effective, with the added advantages of repeatability and robustness. Drop coating was investigated, as the PANI material can be quite difficult to screen print due to the agglomeration of polymer particles causing the screen to clog. Drop coating solves this problem by eliminating the mask entirely.

Gold thick film conductor pastes (Hereaus Materials) were first screen-printed onto pre-cleaned alumina substrates (CeramTec UK Ltd.) to form an interdigitated electrode (IDE) structure. Gold was chosen as it is an inert material and is commonly used in chemical sensing devices. The deposition of the conductor paste was achieved using a DEK 1202 automatic screen printer. The resulting IDE structures were placed into an oven at 80°C for 2 hours to facilitate the initial drying of the pastes. In this oven the remaining solvent in the paste evaporates, leaving the dried pattern on the substrate. The devices are next placed into a furnace for a much higher temperature (850°C) cycle. In this step, any remaining organic binder is removed and the metal frit in the paste is sintered into one solid structure.

This temperature cycle also allows the electrode pattern to settle to its final thickness and resistivity values.

The thick film paste required for deposition is obtained by mixing the required mass of PANI powder (Sigma Aldrich) with 10 wt.% polyvinyl butyral (PVB) (acts as a binder), 10 wt.% surfactant (PS3) (stops the agglomeration of polymer particles) and a suitable amount of ethyleneglycolmonobutylether (solvent). This paste is then screen-printed onto the electrodes. The device is placed into an oven at 80°C for 1.5 hours to facilitate solvent evaporation. Once out of the oven, link wires can be soldered to the bond pads and the devices are ready for testing. Figure. 2 shows a diagram of the resulting sensor, with the pH-sensitive layer deposited over an IDE structure.

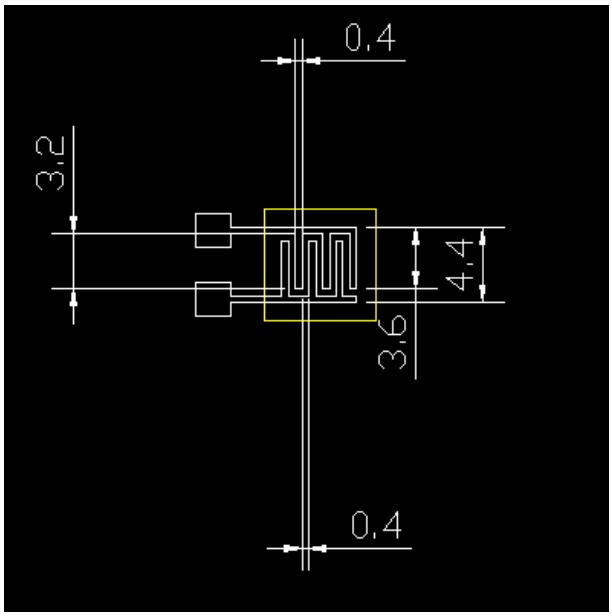

Figure 2. Conductimetric pH sensor using PANI/PVB/PS3 composite material as the pH-sensitive layer (Area outlined by yellow box). All dimensions in the diagram are in mm.

For drop-coated sensor structures, the PANI composite material was prepared by manually mixing 100 mg of ES with 100 mg of polyvinyl butyral (PVB) and 50 mg of hypermer PS3 surfactant. The PVB/ES/surfactant mixture is then added to 20 ml of tetrahydrofuran (THF) and shear mixed at 22,000 r.p.m. for 3 minutes. The shear mixing breaks down the agglomerates of ES particles and disperses them into the PVB polymer. The surfactant is absorbed onto the dispersed ES particles and prevents reagglommeration. A 2 µl drop of the PANI/PVB/PS3 solution was deposited onto the IDE electrode pattern by use of a Transferpette® (Sigma Aldrich) piston operated pipette. The drop is suspended on the pipette tip and is pulled onto the substrate by surface tension. The substrates were then placed into an oven at 80°C for 3 hours to facilitate solvent evaporation. This process was repeated several times to ensure a good polymer film over the electrodes. The reason that a higher amount of PVB is used in drop-coated sensors is due to the poor adherence of the drop-coated films with less than 50 wt.% of PVB in the mixture.

The polymer film thicknesses were measured using a Dektak Surface Profile Measuring System.

The I-V characteristics and DC resistance measurements with temperature were carried out using an in house developed I-V-R profiler, which applies a DC voltage (-14.5 V to +14.5 V) and measures the resulting current. The system is also capable of measuring the resistance directly. The measurements can be made at any temperature between 20°C to 70°C. A National Instruments Data Acquisition (DAQ) card controlled by LabWindows/CVI software and driven by customized electronics hardware measured the IV characteristics of the devices.

Testing is carried out by immersing the sensor into 20 ml of test buffer (obtained from Sigma Aldrich (pH2-pH11)) and recording the change in resistance/conductance. The exact pH and temperature of the buffers is measured using a Hanna HI 991001 pH/Temperature meter. The changes in electrical parameters of the device are recorded using a HP 4192A Low Frequency Impedance Analyzer and a Thurlby Thandar Instruments Tti 1705 Programmable Multimeter. Entire AC analysis is undertaken using a 50 mV r.m.s. signal at the required frequency.

SEM images of the resulting films were obtained using a JEOL JSM-840 Scanning Microscope to examine the morphology of the film and to investigate if this changes due to exposure to the test solutions.

XPS analysis was undertaken using a Kratos AXIS 165 spectrometer with a mono Al K_α X-ray source (1486.6 eV) and a base pressure of 9 x 10^{-10} Torr with a hemispherical analyser. The X-ray source was run at a power of 120 W (10 kV and 12 mA). All binding energies were referenced to the C 1s line of adventitious hydrocarbon peak at 284.6 eV. This analysis was undertaken to observe the changes in the chemical environment of the films due to exposure to solutions of different pH.

3. Results and Discussion

PANI composite films were subjected to a number of tests to establish as much information as possible about the material under investigation. Both DC and AC electrical characteristics were recorded to establish the conduction mechanism of both the thick and drop-coated films. The AC characteristics were obtained over a frequency range of 10 Hz to 10 MHz. The change in the conductance of the films was recorded while the films were in contact with solutions of known pH. This experiment was varied over a number of different time frames and by changing pH directions. XPS analysis was undertaken on films that had been left to soak in different buffers for 3 days to observe the nature of the doping in the films. SEM analysis was also undertaken on these same samples.

3.1. DC and AC Electrical Characteristics

The DC electrical characteristics of the PANI composite films were obtained by applying a sweeping DC voltage (0V to +2 V) to the IDE electrodes, and measuring the resulting current through the film. It was found that the current-voltage characteristics for each film were near-ohmic in the tested voltage range. The films produced by the drop-coating method possessed a much larger resistance than those obtained by the thick film approach. The reason for this is the drop-coating deposition method allows the agglomeration of the particles in the film. The particles are suspended in the solvent/PANI/PVB/PS3 drop on the IDE/substrate surface. Before the solvent evapourates, the PANI particles are free to move within the solvent. As the solvent evapourates, the particles settle in

their final positions. The amount of movement of the particles is dependent on the drop size and also on the evapouration time. As the drop is spread over the IDE surface, there are not enough particles present to create a dense (and thus low resistance) film. Further deposition of the solution results in a more dense film, however, it must be assumed that the majority of the conducting PANI particles settle on top of the previous film and thus limits the amount of contact between the conducting species. Another factor for the high resistivity values of the drop-coated film is the increased amount of PVB binder required to ensure adequate adhesion of the film to the substrate/IDE structure. Approximately 50% of the weight of the composite material is insulating PVB polymer that has the effect of increasing the overall resistance of the film. The screen-printing approach, on the other hand, compresses the particles together into a dense film, thereby creating more conducting paths, resulting in a lower resistance value. The thickness of the drop-coated films are comparable to the thick films, with the 30 x 2 µl film having a thickness of 100 µm and the 10 x 2 µl film having a thickness of 50 µm. Therefore, the resulting current-voltage relationships are offset, and this offset is dependent on the deposition method. This data can be seen in Figure 3.

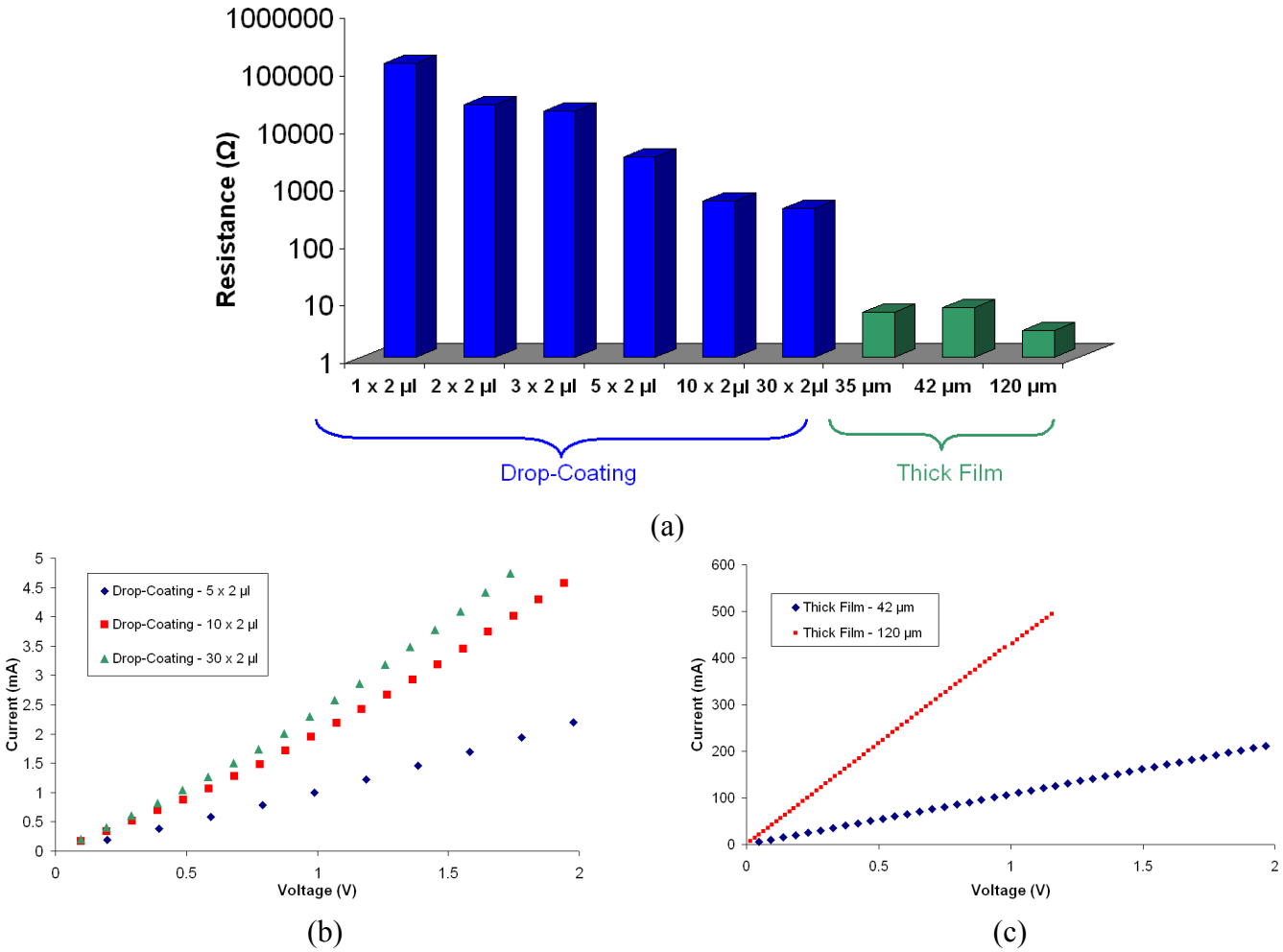

Figure 3. DC electrical characteristics of the various PANI films produced using both drop-coating and thick film deposition, showing: (a) the variation of resistance with deposition method; (b) the current-voltage relationship of the Drop-Coated films; and (c) the current-voltage relationship of the Thick films.

As mentioned previously, the charge carriers in this system are polarons and bipolarons formed during the doping process [29]. However, the DC conductivity in the film depends on these charge carriers being able to travel through the film. Pinto *et al.* [36] described this conductivity in terms of the film being composed of "crystalline regions" (metallic islands) separated by disordered regions. It is the charge transport across these "disordered" regions, which determines the overall DC conductivity of the film. The mechanism for charge transport is referred to by others as a variable-range hopping transport of carriers [37].

The AC electrical characteristics of the films were recorded over the frequency range of 10 Hz to 10 MHz using a sinusoidal signal of 1 V r.m.s. It was found that the conductance of the films remained stable over a wide frequency range (10 Hz to 1 MHz), with the conductance undergoing a decrease in magnitude at frequencies above 1 MHz. The data obtained for the PANI composite films can be seen in Figure 4.

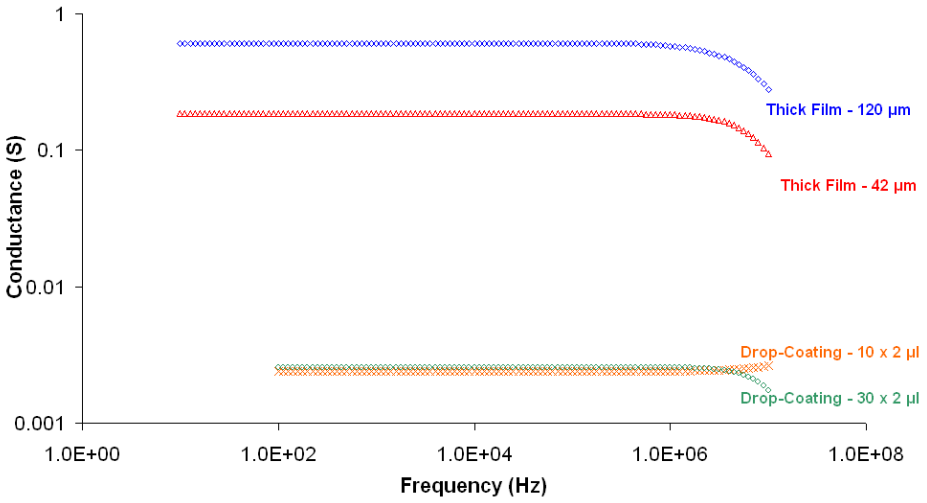

Figure 4. AC electrical characteristics of the various PANI films produced using both drop-coating and thick film deposition, showing conductance values taken over a frequency range of 10 Hz to 10 MHz.

The relationship between AC conductivity and DC conductivity can be explained by the equation:

$$\sigma_{AC} = \sigma_{TOT} - \sigma_{DC} = A\omega^{s} \quad (1)$$

Where, σ_{AC} is the AC conductivity component, σ_{TOT} is the total conductivity, σ_{DC} is the DC conductivity component, A is a complex constant, ω is the angular frequency and s is an index which is characteristic of the type of conduction mechanism/relaxation mechanism dominant in amorphous materials. According to Pollack and Geballe [38], if the value of s lies between 0.5 and 1.0, a hopping conduction is said to dominate. The data presented in Figure 4 is similar to the AC data presented by Saravanan et al. [39] in their paper describing the electrical and structural properties of PANI doped with camphor sulphonic acid, where equation (1) was also used to explain the AC conductivity. They

stated that the activation energy required for hopping processes in materials with higher dielectric permittivity is assumed to be quite low.

Figure 5 shows the results of impedance spectroscopy studies on films fabricated using both deposition methods. It can be seen that the conduction in the thick film sample follows a different trend to that in the drop-coated sample. The main reason behind this is that in the drop-coated samples, there is a larger amount of the insulating phase (PVB) and that at higher frequencies carriers are required to traverse this region resulting in a decrease in impedance at higher frequencies. This is represented in Figure 5 (a) with a decrease in the real part component of impedance (Re (Z)) with a corresponding increase in the imaginary part component (Im (Z)). For the screen-printed thick films, on the other hand, the particles are in much closer proximity, with the insulating phase almost negligible. Figure 5 (b) shows that neither the real nor the imaginary component changes by a large amount as the frequency increases.

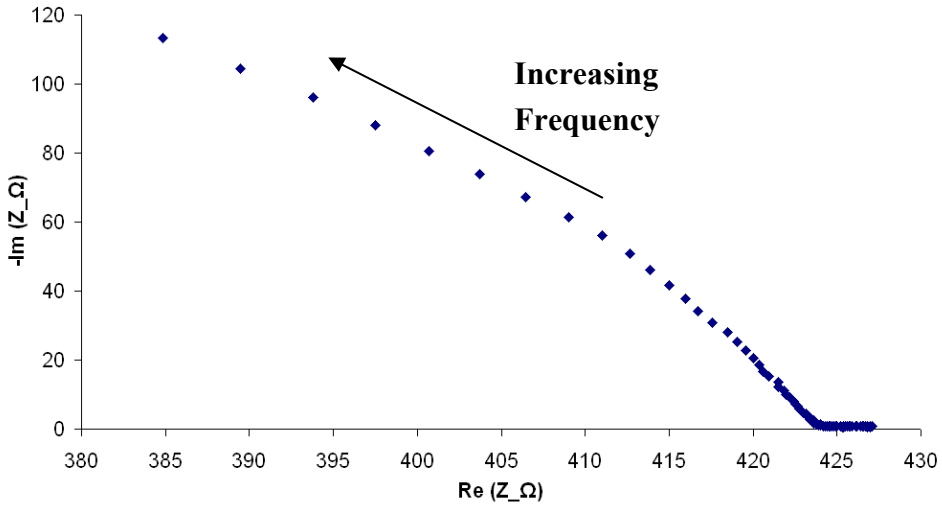

(a)

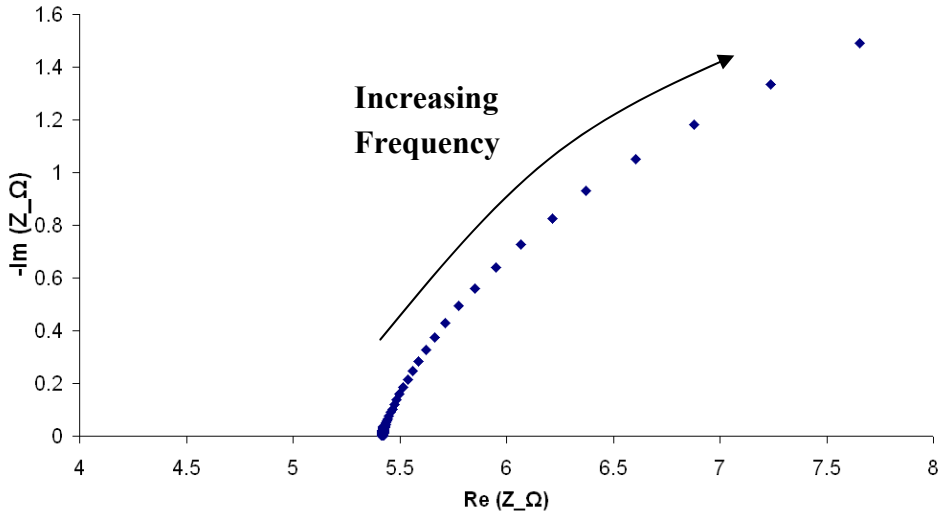

(b)

Figure 5. Impedance Spectroscopy of PANI/PVB/PS3 composite films fabricated using (a) Drop-Coating; and (b) Thick Film.

3.2. XPS analysis of PANI Composite Films

X-ray photoelectron spectroscopy (XPS) was carried out on 120 µm PANI composite thick films to investigate the reaction mechanisms involved in the conductance change in the film due to the pH of the test buffer. Films were immersed in the pH buffers over 96 hours and then analysed using XPS. Figure 6 shows the data obtained from the analysis over the full range of binding energies, while Figure 7 shows the XPS data generated for the 6 films used for this experiment, showing the N 1s spectra obtained.

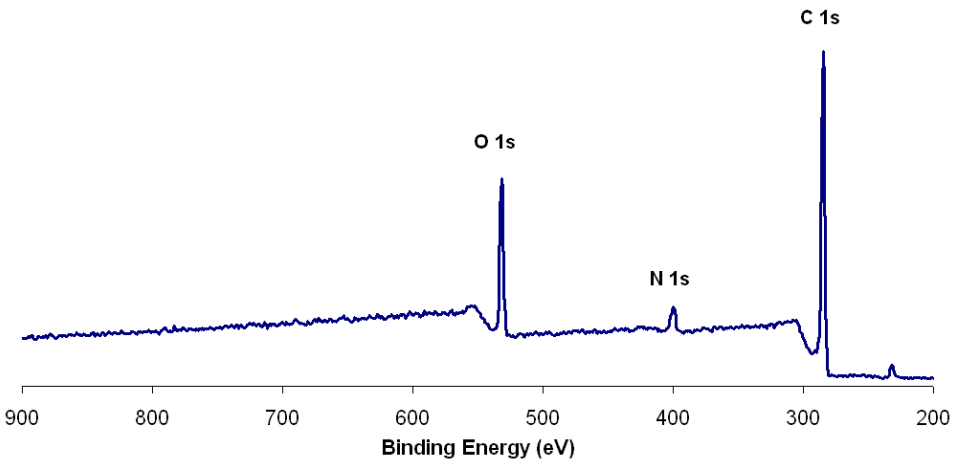

Figure 6. XPS survey spectra showing the data gathered for the PANI/PVB/PS3 composite film over the full range of binding energies investigated.

The resulting XPS data reveals the reaction mechanism between the PANI composite films and the buffer solutions used in the experiments. For the untested film, as seen in Figure 7 (a), and the two films soaked in acidic buffers, shown in Figure 7 (b) and (c), it can be seen that there are three main contributions to the curve. The first peak, in this case, is generally attributed to the amine nitrogen (─NH─) at 399.4 eV [40]. The other two smaller peaks can be attributed to positively charged nitrogen (N^+) and are located at 400.5 eV and 402.2 eV respectively [41]. A noticeable change in the N 1s spectra can be seen for the films soaked in the pH6 buffer, shown in Figure 7 (d), and the two alkaline buffers (pH8 and pH10), shown in Figure 7 (e) and (f). In addition to the three contributions observed in films soaked in acidic solutions, an additional peak can be seen, which can be attributed to imine nitrogen (=N─) at 398.1 eV. The imine nitrogen peak intensity increases with increasing pH, while the N^+ peaks decrease in intensity. This shows that the varying conductivity of the films in solutions of different pH is due to the protonation/deprotonation of the backbone of the PANI material. Table 1 summarizes the findings of the XPS analysis on the 120 µm PANI composite thick films.

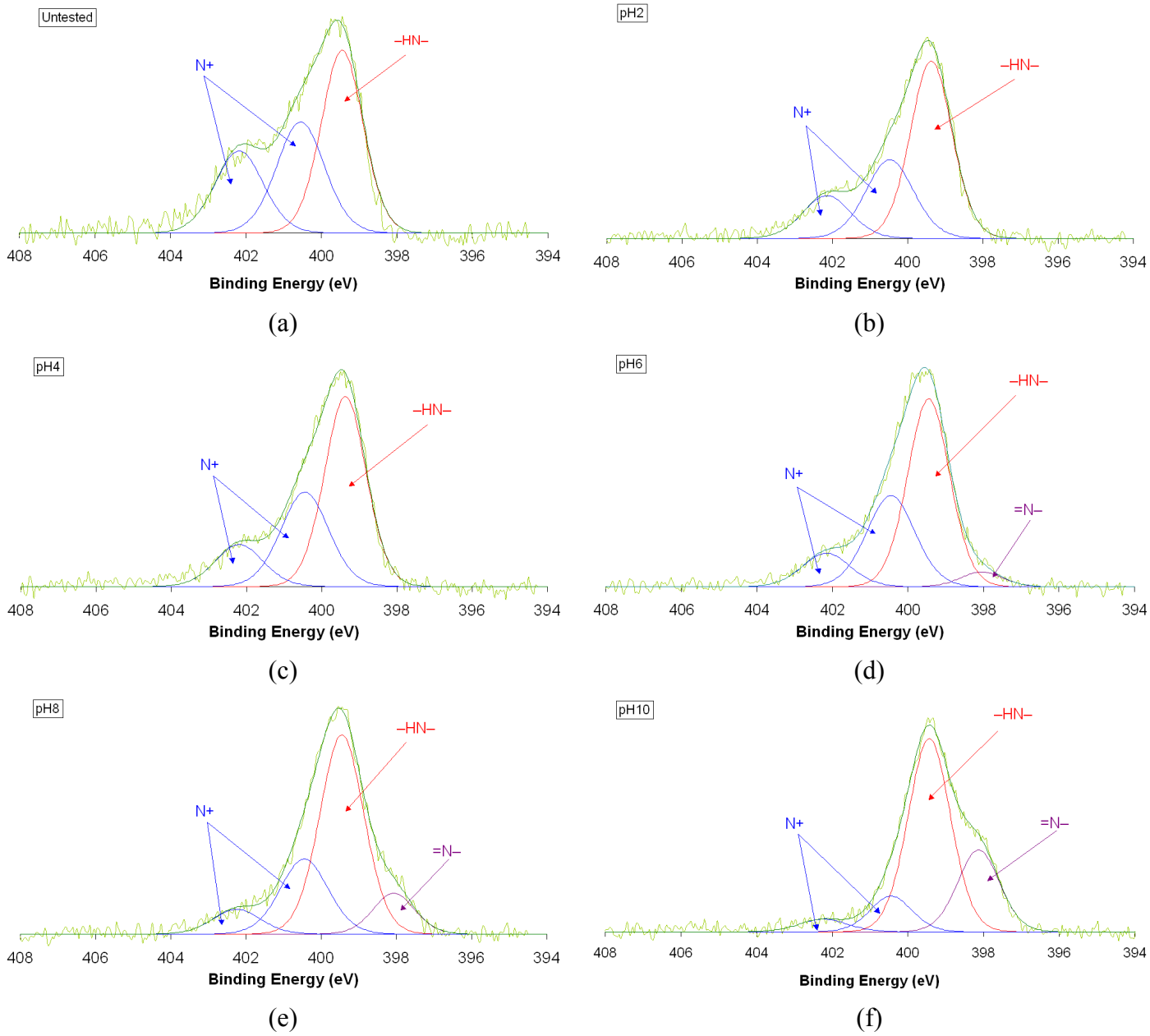

Figure 7. XPS spectra (N 1s) of 120 µm PANI composite thick films tested over 96 hours showing: (a) untested film; (b) film soaked in pH2 buffer; (c) film soaked in pH4 buffer; (d) film soaked in pH6 buffer; (e) film soaked in pH8 buffer; and (f) film soaked in pH10 buffer.

The data presented in Table 1 shows the calculated ratio for imine to amine nitrogen intensities. This data shows how the ratio is non-existent in protonated films, due to the absence of imine nitrogen, and shows how this ratio increases with pH values greater than pH6.

Table 1. Data from XPS N 1s spectra obtained from 120 μm PANI composite thick films.

Sample #	Test/Duration	=N–	–NH–	N^+	N^+	(=N–)/(–NH–)
1	No Test	0.0	45.1	31.5	23.4	0.0
2	pH2/96 h	0.0	54.3	30.6	15.1	0.0
3	pH4/96 h	0.0	54.5	31.7	13.8	0.0
4	pH6/96 h	4.1	53.9	31.5	10.5	0.076
5	pH8/96 h	11.0	57.6	23.9	7.5	0.191
6	pH10/96 h	25.5	59.5	11.0	4.0	0.38

3.3. SEM analysis of PANI Composite Films

SEM analysis was undertaken for both drop-coated and thick film PANI composite films. Although the change in conductivity of the films due to buffers of different pH value cannot be directly observed by SEM analysis, other factors, such as morphological changes in the film, can be investigated.

It is well known that while the conducting (doped) form of PANI (emeraldine salt) is insoluble in most common solvents, the non-conducting (undoped or deprotonated) form (emeraldine base) is soluble in most common solvents [42]. Therefore, several samples of different PANI/PVB/PS3 composite films were prepared to investigate the possible effects of buffer pH on the degradation of film stability, due to the polymer particles dissolving and, thus, losing adherence to the substrate/electrode structure.

The first films to be investigated were the drop-coated PANI composite films (30 x 2 μl). Although the sensors showed a stable response over 12 hours of testing, after this time it was noted that there was some mechanical degradation of the film. Some portions of the film lost adherence to the substrate and separated completely from the electrodes. It was thought that this was due to the particles dissolving in the test buffers and subsequently lifting off the substrate. However, SEM analysis confirmed that the observed mechanical degradation was not due to the reason envisioned, and was instead due to the polymer binder being unable to retain the particles in the cast film. The main factor behind this mechanical failure is due to the deposition method, which does not distribute the PANI composite material uniformly and thus creates weakened sections of the film. An SEM image of one of the 30 x 2 μl drop coated PANI/PVB/PS3 films can be seen in Figure 8 (a).

The thick films, on the other hand, were far more mechanically stable than their drop-coated counterparts. Screen-printing ensures a homogeneous film and a micrograph of an untested 120 μm screen-printed PANI/PVB/PS3 film can be seen in Figure 8 (b). SEM micrographs were taken for the same films employed in the XPS analysis to observe any possible changes in morphology due to the pH of the test buffers. Profilometry was also undertaken on the films before and after tests but showed that no significant swelling or contraction of the films took place.

The SEM micrographs showed that no discernable changes can be directly attributed to a particular buffer and thus the mechanical changes in the film cannot be caused by the buffer interactions with the PANI functional material. The response of the film to changing pH remained excellent over 96 hours, however, after this time, the adhesion of the films to the IDE/substrate began to degrade. As in the case

of the drop-coated films, SEM analysis showed that it was not the PANI material that was responsible for this loss in adherence, and is attributed to the PVB polymer binder.

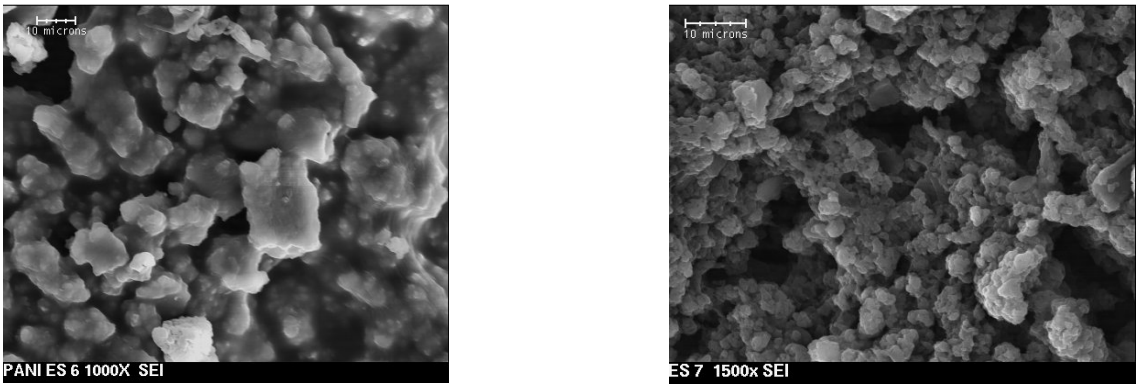

(a) (b)

Figure 8. SEM micrographs showing: (a) drop-coated (30 x 2 µl) PANI/PVB/PS3 composite film; and (b) Screen-printed 120 µm thick PANI/PVB/PS3 composite film.

The apparent difference in particle size between the drop-coated and thick films is due to the increased amount of PVB in the drop-coated method, which appears to cause smaller particles to join together to form larger particles, overcoming the effects of the surfactant. Also, the mask involved in the screen-printing process will stop larger particles from being deposited.

3.4. Effect of pH on Film Conductance

Several films of this novel PANI/PVB/PS3 composition were tested for pH sensitivity. The device was either submerged in 20 ml of buffer (known pH value) or a suitable amount of the same buffer was dropped onto the film surface, and the resulting change in conductance was recorded. It was found that the PANI/PVB/PS3 composite films exhibit a very strong correlation between the film conductance and the buffer pH. The drop-coated films did not produce results of the same caliber of the thick film devices. However, the resistances of these films were measured after each test and this resistance was found to have the same relationship to pH as seen with the thick film devices.

The first series of experiments involved the testing of several drop-coated films. The films investigated were obtained by depositing 10 x 2 µl and 30 x 2 µl drops of PANI composite solution onto the IDE patterns. The change in conductance was recorded when the films were in contact with each buffer, and also when the film was removed from the solution and dried. This enabled the investigation of the permanent effects of the solution pH on the conductance of the PANI composite films. The data obtained from these experiments can be seen in Figure 9.

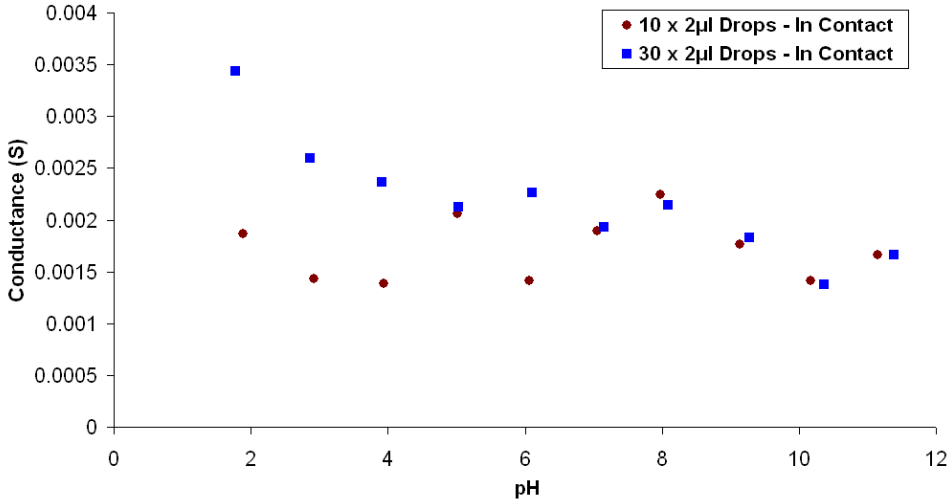

(a)

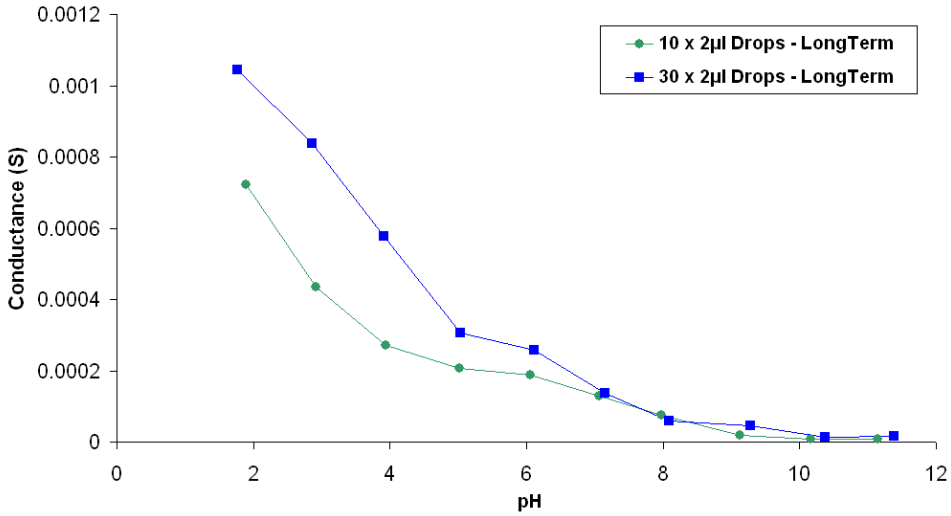

(b)

Figure 9. Plots showing the change in conductivity of PANI composite films when films are: (a) in contact with the test solution; and (b) after rinsing in de-ionised water and drying, showing long term effects of solution pH on film conductance.

From the data presented in Figure 9, it can be seen that while the long-term relationship between conductance and pH follows the expected trend (as explained earlier) of decreasing in magnitude with increasing pH (Figure 9 (b)), the trend observed while the films are in contact with the buffers is not so clear (Figure 9 (a)). The 30 x 2 µl films produced better results in both experiments as there was a superior quality of film over the electrodes and thus the problems encountered with the previous film were eliminated. However, it was noted that after testing, the mechanical stability of the drop-coated films degraded by a considerable amount. Therefore, this deposition method is not ideal for fabricating pH-sensing devices.

The screen-printed thick films investigated, on the other hand, produced much better results when compared to those obtained from the drop-coated films as there were more PANI particles for the solution to interact with. Although of comparable thickness to drop-coated films, the screen-printed films were more uniform over the entire electrode structure, therefore contributing to more stable

results. Also, the mechanical stability was better in the thick films as the particle density was higher, a direct result of the deposition process. The data obtained from the thick PANI composite films can be seen in Figure 10.

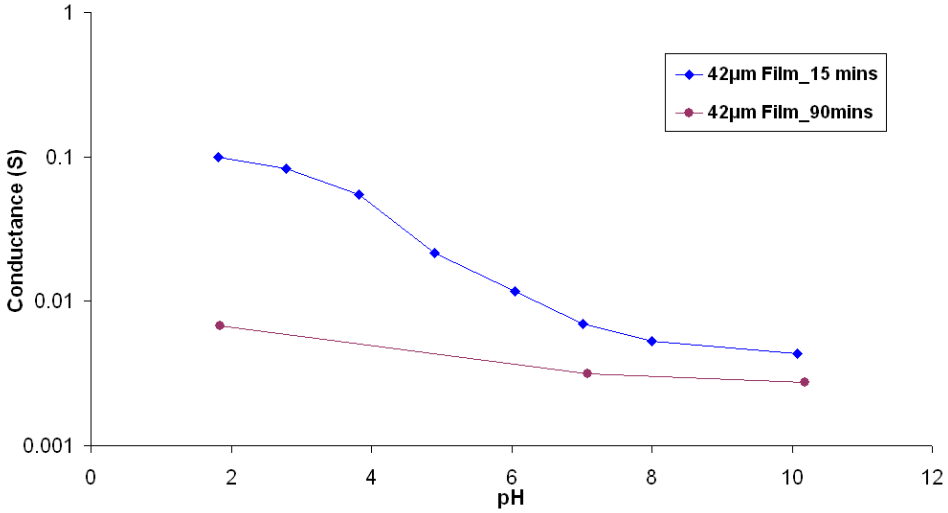

(a)

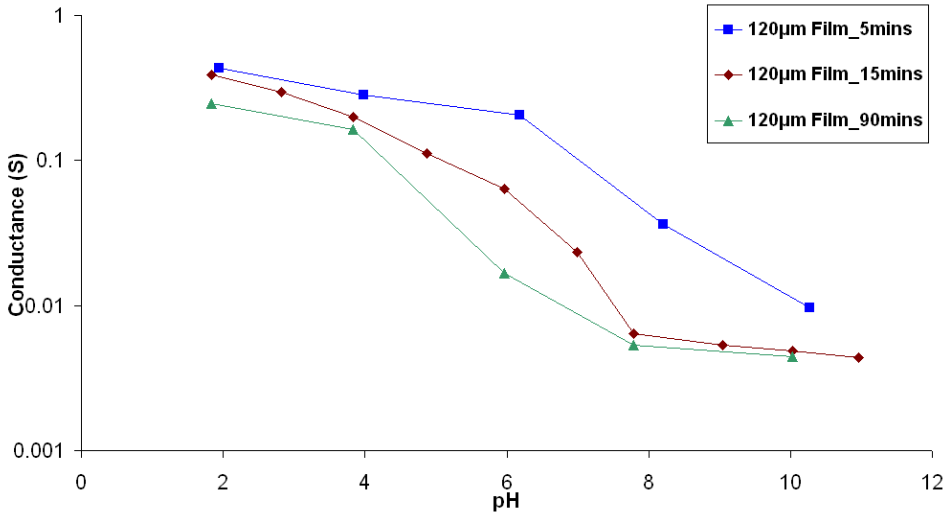

(b)

Figure 10. Plots showing the change in conductivity of PANI composite thick films when films are in contact with the test solutions for (a) 42 µm; and (b) 120 µm thick films.

Films of two thicknesses were investigated in these experiments. The reason for this was to ascertain if the film thickness has any effect on the pH-sensitivity of the films, as it has already been observed (Figure 3) that the thickness directly affects the resistance of the film. Also, each film was tested for different time intervals, to see if there is a correlation between the film conductance and the length of time the film is in contact with the solution. Films of greater thickness have a higher conductivity, however, the response of films of both thicknesses were comparable. It was noticed that after 5 minutes, there was considerable deprotonation of the films, leading to a loss in conductivity. The longer time intervals of 15 minutes and 90 minutes, show that the longer time exposed to a solution, the more protonation/deprotonation takes place. The response of each film was recorded over

time to observe the effects taking place in the film from the instant of exposure to test solutions. Figure 11 shows a sample of this data taken from a 120 µm film exposed to each buffer for 90 minutes.

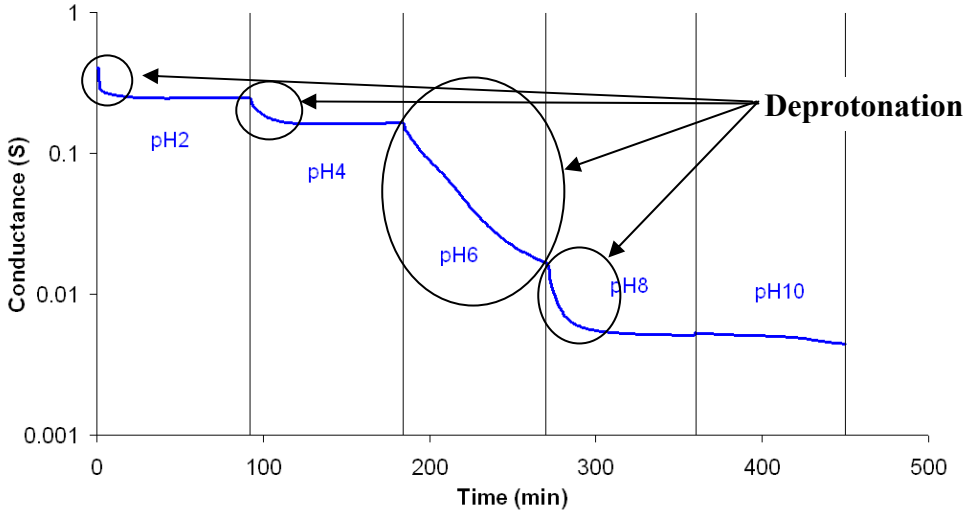

Figure 11. Plot showing the change in conductance of 120 µm PANI composite thick films when films are in contact with the test solutions for 90 minutes.

Slight deprotonation can be observed immediately upon contact with pH2 buffer solution, after which the conductance of the film settles to a stable value. When the film is moved into a buffer with a pH value of 4, a similar trend occurs with an initial deprotonation of the film, followed by a stabilizing of the conductance value of the film. Once the film is introduced to the pH6 buffer, a much larger deprotonation process takes place (pH6 buffer is an almost neutral solution), and the conductance of the film decreases considerably. Next the film is moved into alkaline solutions, where the final deprotonation of the film takes place. By the time the film is placed into the pH10 buffer, most of the film has already been deprotonated, however, the excess amount of hydroxide ions in this solution causes the removal of most of the remaining amine hydrogen, which decreases the conductance of the film even further.

4. Conclusions

In this paper we have reported on the pH sensitivity of a novel PANI/PVB/PS3 composite film. It was found that although drop-coated PANI composite films are not suitable for in-situ pH measurement, they did show doping effects due to the varying pH of the test solutions. Screen-printed PANI composite thick films did, on the other hand, show excellent response to pH change both in contact with the test solutions and also showed permanent doping effects. The reaction mechanism for this pH sensitivity was shown to be due to the protonation/deprotonation of the films, which is proportional to the pH of the solution, and this was supported by XPS analysis. SEM micrographs along with Profilometry showed that no physical changes occurred in the films due to exposure to the various test buffers. PANI/PVB/PS3 composite films show excellent pH sensitivity, with the conductance of the films varying by as much as three orders of magnitude over the pH range of pH2 – pH11. The device response was stable over 96 hours testing. It may be possible to improve on this time frame by improving the adherence of the films to the substrate/IDE pattern.

Acknowledgements

This research was supported by the Irish Research Council for Science, Engineering and Technology (IRCSET): Funded by the National Development Plan.

References

1. Göpel, W.; Jones, T. A.; Kleitz, M.; Lundström, J; Seiyama, T. In *Chemical and Biochemical Sensors*; Göpel, W., Hesse, J. and Zemel, J. N., Ed.; VCH: New York, 1991.
2. Lakard, B.; Herlem, G.; Labachelerie, M.; Daniau, W.; Martin, G.; Jeannot, J.-C.; Robert, L; Fahys, B. Miniaturized pH Biosensors Based on Electrochemically Modified Electrodes with Biocompatible Polymers. *Biosensors and Bioelectronics* **2004**, *19*, 595-606.
3. Lakard, B.; Herlem, G.; Lakard, S.; Guyetant, R.; Fahys, B. Potentiometric pH sensors based on electrodeposited polymers. *Polymer* **2005**, *46*, 12233-12239.
4. Kang, T.-F.; Xie, Z.-Y.; Tang, H.; Shen, G.-L.; Yu, R.-Q. Potentiometric pH Sensors Based on Chemically Modified Electrodes with Electropolymerized Metal-Tetraaminophthalocyanine. *Talanta* **1997**, *45*, 291-296.
5. Adhikari, B.; Majumdar, S. Polymers in sensor applications. *Progress in Polymer Science* **2004**, *29*, 699-766.
6. Hailin, G.; Yucheng, L. Characterization of a chemoresistor pH sensor based on conducting polypyrrole. *Sensors and Actuators B: Chemical* **1994**, *21*, 57-63.
7. Korostynska, O.; Arshak, K.; Gill, E.; Arshak, A. Review on State-of-the-art in Polymer Based pH Sensors. *Sensors* **2007**, *7*, 3027-3042.
8. Chandrasekhar, P. *Conducting Polymers, Fundamentals and Applications: A Practical Approach*; Kluwer Academic Publishers: Boston, 1999.
9. Mo, X.; Wang, J.; Wang, Z.; Wang, S. Potentiometric pH responses of fibrillar polypyrrole modified electrodes. *Sensors and Actuators B: Chemical* **2003**, *96*, 533-536.
10. Lakard, B.; Segut, O.; Lakard, S.; Herlem, G.; Gharbi, T. Potentiometric miniaturized pH sensors based on polypyrrole films. *Sensors and Actuators B: Chemical* **2007**, *122*, 101-108.
11. De Marcos, S.; Wolfbeis, O. S. Optical sensing of pH based on polypyrrole films. *Analytica Chimica Acta* **1996**, *334*, 149-153.
12. Jin, Z.; Su, Y.; Duan, Y. An improved optical pH sensor based on polyaniline. *Sensors and Actuators B: Chemical* **2000**, *71*, 118-122.
13. Talaie, A. Conducting polymer based pH detector: A new outlook to pH sensing technology. *Polymer* **1997**, *38*, 1145-1150.
14. Letheby, H. On the production of a blue substance by the electrolysis of sulphate of aniline. *Journal of the Chemical Society* **1862**, *15*, 161.
15. Shan, D.; Wang, S.; He, Y.; Xue, H. Amperometric glucose biosensor based on in situ electropolymerized polyaniline/poly(acrylonitrile-co-acrylic acid) composite film. *Materials Science and Engineering: C. In Press, Corrected Proof.*
16. Xian, Y.; Hu, Y.; Liu, F.; Xian, Y.; Wang, H.; Jin, L. Glucose biosensor based on Au nanoparticles-conductive polyaniline nanocomposite. *Biosensors and Bioelectronics* **2006**, *21*, 1996-2000.

17. Pan, X.; Kan, J.; Yuan, L. Polyaniline glucose oxidase biosensor prepared with template process. *Sensors and Actuators B: Chemical* **2004**, *102*, 325-330.
18. Castillo-Ortega, M. M.; Del Castillo-Castro, T.; Ibarra-Bracamontes, V. J.; Nuno-Donlucas, S. M.; Puig, J. E.; Herrera-Franco, P. J. Urea sensing film prepared by extrusion from DBSA-doped polyaniline-poly(styrene-co-potassium acrylate) in a poly(n-butyl methacrylate) matrix. *Sensors and Actuators B: Chemical* **2007**, *125*, 538-543.
19. Arora, K.; Sumana, G.; Saxena, V.; Gupta, R. K.; Gupta, S. K.; Yakhmi, J. V.; Pandey, M. K.; Chand, S.; Malhotra, B. D. Improved performance of polyaniline-uricase biosensor. *Analytica Chimica Acta* **2007**, *594*, 17-23.
20. Luo, Y.-C.; Do, J.-S. Urea biosensor based on PANi(urease)-Nafion(R)/Au composite electrode. *Biosensors and Bioelectronics* **2004**, *20*, 15-23.
21. Dhand, C.; Singh, S. P.; Arya, S. K.; Datta, M.; Malhotra, B. D. Cholesterol biosensor based on electrophoretically deposited conducting polymer film derived from nano-structured polyaniline colloidal suspension. *Analytica Chimica Acta*. *In Press, Accepted Manuscript*.
22. Singh, S.; Solanki, P. R.; Pandey, M. K.; Malhotra, B. D. Covalent immobilization of cholesterol esterase and cholesterol oxidase on polyaniline films for application to cholesterol biosensor. *Analytica Chimica Acta* **2006**, *568*, 126-132.
23. Singh, S.; Solanki, P. R.; Pandey, M. K.; Malhotra, B. D. Cholesterol biosensor based on cholesterol esterase, cholesterol oxidase and peroxidase immobilized onto conducting polyaniline films. *Sensors and Actuators B: Chemical* **2006**, *115*, 534-541.
24. Dixit, V.; Tewari, J. C.; Sharma, B. S. Detection of E. coli in water using semi-conducting polymeric thin film sensor. *Sensors and Actuators B: Chemical* **2006**, *120*, 96-103.
25. Lindfors, T.; Ivaska, A. pH sensitivity of polyaniline and its substituted derivatives. *Journal of Electroanalytical Chemistry* **2002**, *531*, 43-52.
26. Huang, W. S.; Humphrey, B. D.; MacDiarmid, A. G. Polyaniline, a novel conducting polymer. Morphology and chemistry of its oxidation and reduction in aqueous electrolytes. *Journal of the Chemical Society, Faraday Transactions 1: Physical Chemistry in Condensed Phases* **1986**, *82*, 2385-2400.
27. MacDiarmid, A. G. In *The polyanilines: A novel class of conducting polymers*; Salaneck, W. R., Lundström, I.; Rånby, B., Ed.; Oxford University Press: Oxford, 1993.
28. Stejskal, J.; Gilbert, R. G. Polyaniline, Preparation of a Conducting Polymer. *Pure Applied Chemistry* **2002**, *74*, 857-867.
29. Brédas, J.-L. In *The Polyanilines: Illustration of the interconnection between chemical structure, geometric structure, and electronic structure in conjugated polymers*; Salaneck, W. R., Lundström, I. and Rånby, B., Ed.; Oxford University Press: Oxford, 1993.
30. Luthra, V.; Singh, R.; Gupta, S. K.; Mansingh, A. Mechanism of dc conduction in polyaniline doped with sulfuric acid. *Current Applied Physics* **2003**, *3*, 219-222.
31. Ray, A.; Richter, A. F.; MacDiarmid, A. G.; Epstein, A. J.; Polyaniline: protonation/deprotonation of amine and imine sites. *Synthetic Metals* **1989**, *29*, 151-156.
32. Lindfors, T.; Ervela, S.; Ivaska, A. Polyaniline as pH-sensitive component in plasticized PVC membranes. *Journal of Electroanalytical Chemistry* **2003**, *560*, 69-78.

33. Lindfors, T.; Harju, L.; Ivaska, A. Optical pH Measurements with Water Dispersion of Polyaniline Nanoparticles and Their Redox Sensitivity. *Anal. Chem.* **2006**, *78*, 3019-3026.
34. Lindfors, T.; Ivaska, A. Raman based pH measurements with polyaniline. *Journal of Electroanalytical Chemistry* **2005**, *580*, 320-329.
35. Lindfors, T.; Ivaska, A. Application of Raman Spectroscopy and Sequential Injection Analysis for pH Measurements with Water Dispersion of Polyaniline Nanoparticles. *Anal. Chem.* **2007**, *79*, 608-611.
36. Pinto, N. J.; Shah, P. D.; McCormick, B. J.; Kahol, P. K. Dependence of the conducting state of polyaniline films on moisture. *Solid State Communications* **1996**, *97*, 931-934.
37. Moon Gyu Han, S. S. I. Dielectric spectroscopy of conductive polyaniline salt films. *Journal of Applied Polymer Science* **2001**, *82*, 2760-2769.
38. Pollack, M.; Geballe, T. H. Low-frequency conductivity due to hopping processes in silicon. *Physical Review* **1961**, *122*, 1742-1753.
39. Saravanan, S.; Joseph Mathai, C.; Anantharaman, M. R.; Venkatachalam, S.; Prabhakaran, P. V. Investigations on the electrical and structural properties of polyaniline doped with camphor sulphonic acid. *Journal of Physics and Chemistry of Solids* **2006**, *67*, 1496-1501.
40. Rodrigues, P. C.; Muraro, M.; Garcia, C. M.; Souza, G. P.; Abbate, M.; Schreiner, W. H.; Gomes, M. A. B. Polyaniline/lignin blends: thermal analysis and XPS. *European Polymer Journal* **2001**, *37*, 2217-2223.
41. Jousseaume, V.; Morsli, M.; Bonnet, A.; Lefrant, S. Electronic structure of conducting polyaniline blends. *Optical Materials* **1998**, *9*, 480-483.
42. Sanchis, C.; Salavagione, H. J.; Arias-Pardilla, J.; Morallon, E. Tuning the electroactivity of conductive polymer at physiological pH. *Electrochimica Acta* **2007**, *52*, 2978-2986.